Computer Fraud and Security
ISSN (online): 1873-7056

Multi-view Graph Learning based Progression Modeling of Parkinson's Disease Using Whole-blood Transcriptomics Data

Zeqi Xu
Zhejiang Sci-Tech University
Corresponding Email：202230603130@mails.zstu.edu.cn

Abstract: In human disease modeling, blood transcriptomics data has played a crucial role in revealing regulatory abnormality. As patterns underlying blood transcriptomics data are subtle, it is insufficient to rely on temporal expression features to predict future stages of brain diseases. Spatial features have encoded meaningful information about gene-level and cell-level interactions. Progression of neurological disorder lasts 10-15 years, indicating that disease-specific gene graphs are changing. In order to employ dynamic spatial features, this work proposes a novel dynamic spatiotemporal graph learning (DST-GNN) to conduct disease progression prediction. The DST-GNN method aims to integrate expression patterns and dynamic gene graphs. Validation experiments about benchmark whole-blood RNA-seq datasets from the AMP-PD platform have demonstrated the effectiveness and advantages of the DST-GNN.

Keywords: blood transcriptomics; spatial features; dynamic gene graphs; temporal expression features

1. INTRODUCTION

In precision medicine, it is important to recognize disease stages accurately. There are multiple types of biomedical dataset that can be used to conduct disease modeling. Among these datasets, gene expression data have played a crucial role. Previous works have investigated changes of gene expression levels to conduct molecular diagnosis. However, this is not accurate due to lack of deep-level representations.

Compared with brain expression data [1]-[3], transcriptomic data measured from blood samples is extremely complicated and contain limited information. Traditional pattern recognition approaches [4]-[6] face difficulty in extracting and detecting meaningful patterns from blood expression data [7],[8]. With development of powerful deep learning models, it has became feasible to evaluate the process of dementia and cognitive decline from the subtle changes of blood expression levels. Such investigation may involve dysfunction of immune systems.

In this case, spatial features could be useful in boosting performance and reliability diagnositic models. As it reflect structural changes or topological changes at the molecular level. For instance, gene network are inferred to capture meaningful changes of regulatory systems. It is noted that static gene graphs encode regulatory information at a specific time snapshot. Dynamic gene networks, which were inferred at multiple disease stages, have the potential to describe disease progression. Motivated by this, dynamic gene networks are inferred to get deep-level representations about disease states [9].

For pattern recognition approaches in biomedical model [10], graph neural network have been widely used in recognize meaningful patterns. Among multiple GNN derivatives, dynamic GNN has enhanced capabilities to capture meaningful patterns from omics data. More impotantly, multi-view learning technology offer the possibility of integrating temporal expression dynamics and gene graphs.

With the support of dynamic gene graphs, a novel spatial-temporal graph learning framework has been proposed to deal with PD progression modeling. Using blood transcriptomics data as a training set, a dynamic GNN has played the backbone in assessing disease states as well as motor dysfunction.

The contributions of this study are summarized as follows:

- Spatial features of gene networks have been taken into account in disease modeling.
- A dynamic spatial graph neural network was designed to capture dynamic spatial features and improve the performance of the model.
- A Dual-Channel Transformer model framework was designed to integrate spatiotemporal (ST) representations. The Kolmogorov-Arnold Networks (KAN) model was used as a classifier to enhance nonlinear modeling capabilities.

2. RELATED WORKS

2.1 Inference of gene network graphs

Gene network analysis is a crucial method for uncovering the complex relationships between genes, exploring biological mechanisms, and identifying the underlying patterns of disease onset and progression. At present, various methods have been widely applied to the construction and analysis of gene networks. WGCNA [11] is a classical approach that constructs weighted networks by calculating correlations between gene expressions, identifies co-expression modules, and associates them with phenotypic traits. However, WGCNA primarily focuses on static networks, making it challenging to capture the changes in networks during dynamic biological processes. To address this limitation, MEGENA [12] was proposed. By employing multiscale embedded analysis, MEGENA reveals hierarchical and topological structures within gene networks, making it more suitable for analyzing complex biological systems.

In recent years, deep learning techniques have also been introduced into the field of gene network inference. For instance, DeepTFni [13] is a deep neural network-based approach that focuses on identifying regulatory relationships between transcription factors and their target genes. By integrating gene expression and multi-omics data, DeepTFni significantly improves the accuracy of regulatory network predictions; however, its robustness in noisy data environments requires further optimization. On the other hand, PySCENIC [14], as a comprehensive toolkit, combines motif analysis based on transcription factor binding sites with co-expression network inference. This enables the simultaneous identification of transcription factors' direct target genes and their regulatory networks.

2.2 Dynamic Graph Neural Networks

In the context of temporal tasks, Dynamic Graph Neural Networks (DGNNs) [15] have become an important research direction in recent years, particularly in tasks that require capturing both graph structure and temporal evolution features, demonstrating superior performance. Traditional static Graph Neural Networks (GNNs) [16] primarily rely on fixed graph structures and node features, making it difficult to effectively handle temporal changes. However, DGNNs address this challenge by introducing a temporal dimension, enabling dynamic updates of node and edge features in the graph to adapt to time-varying conditions. For instance, CTGCN [17] introduces a dynamic graph neural network architecture based on a gating mechanism, which effectively captures the temporal and spatial dependencies by integrating temporal information with Graph Convolutional Networks (GCNs). ASTGCN [18], on the other hand, incorporates an attention mechanism to adaptively learn the spatial relationships between different nodes and the temporal dependencies between different time steps, overcoming the limitations of fixed weights in traditional methods and allowing the model to dynamically adjust its focus based on the specific characteristics of the data. DGCNN [19] presents a network architecture that combines dynamic graphs with spatiotemporal convolutions, effectively capturing the dynamic characteristics of traffic flow over time while adaptively modeling the spatial structure, thus overcoming the limitations of traditional methods that cannot simultaneously handle spatiotemporal dependencies.

2.3 Multi-view Learning

Multiview Learning [20]-[22] integrates data from different perspectives, enabling a more comprehensive understanding of the underlying structure and relationships within the data. It strengthens the complementarity between various perspectives, thereby facilitating the model’s thorough understanding of the data features. Traditional multiview learning methods mainly focus on how to effectively fuse information from different perspectives, such as through weighted fusion or feature-level fusion strategies. However, these methods often face challenges related to inconsistencies between perspectives and information redundancy, making it difficult to preserve the effectiveness of the information while avoiding the interference of redundant data.

In multiview learning frameworks, deep neural networks, through information sharing and cross-modal learning, can automatically extract effective features from different perspectives and optimize and fuse these features. For example, the multiview learning approach based on Graph Attention Networks [23] enhances the model's discriminative ability by processing images from different perspectives. MAET [24] introduces a novel multimodal adaptive emotion transformer, which can flexibly handle inputs from multiple perspectives. TNNLS

[25] combines multi-task learning and multiview learning in the field of graph representation learning, achieving better performance.

3. THE PROPOSED DST-GNN METHOD

In order to conduct high-quality disease progression prediction model, this work proposes dynamic spatiotemporal graph learning architecture (DST-GNN) to integrate dynamic spatial features about gene networks, under the framework of multi-view learning. The model framework is shown in Fig 1. In this work, gene graphs play the role of spatial features. Specifically, spatiotemporal learning framework is employed to integrate temporal expression patterns and spatial features.

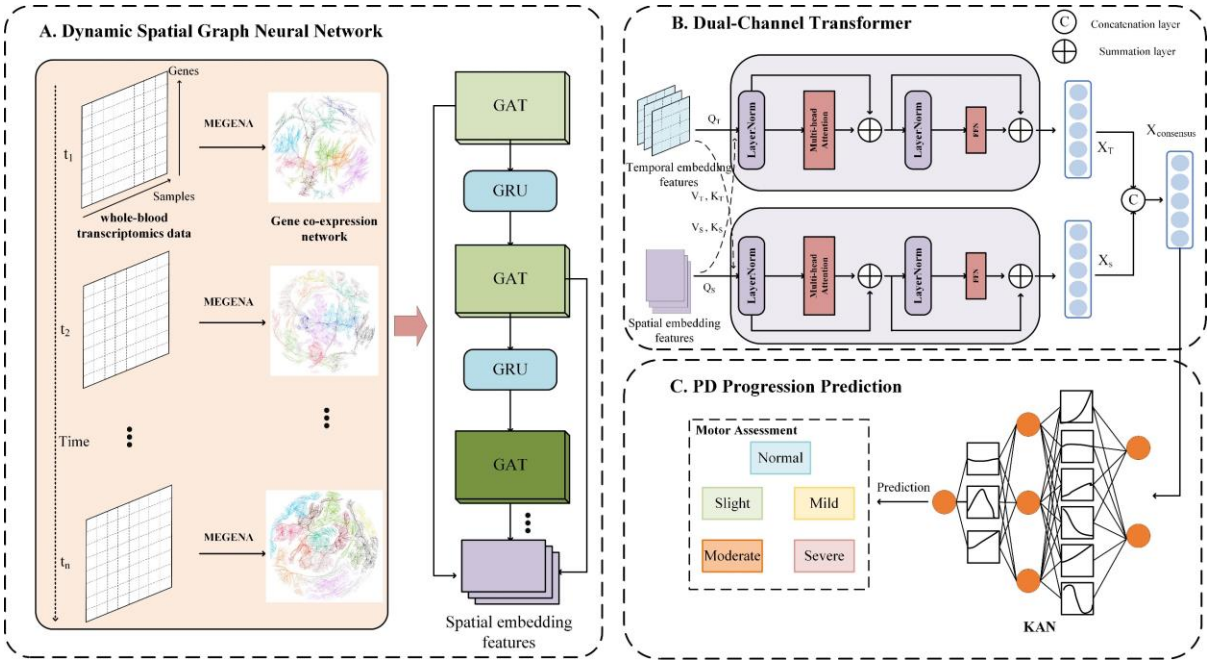

Fig 1: The overview of DST-GNN method. The gene co-expression network represents spatial data, while the blood transcriptomics data corresponds to temporal data. A dynamic spatial GNN model is employed to integrate dynamic spatial information, followed by a dual-channel Transformer model to jointly model both spatial and temporal information, thereby obtaining a rich spatiotemporal representation. The KAN layer is subsequently applied for feature transformation, further enhancing the model's nonlinearity.

3.1 Inference of dynamic gene graphs

During computational modeling of disease dynamics, genes expression levels contribute to a temporal perspective. For blood transcriptomics, changes of gene expression levels are subtle. In order to enhance the predictive accuracy, deep-level representations are necessary. In this case, dynamic gene networks could contribute to a more powerful progression prediction model.

The data from the past *t* time steps are used to predict the disease severity at time step *t+1*. In the whole blood transcriptomics data, the gene expression data *X* at each time snapshot consists of *m* patients and *n* genes. To construct a dynamic gene atlas, the MEGENA algorithm is employed to infer the gene co-expression network [26]-[28] for Parkinson's disease (PD-GCN).

$$r_{ij} = \frac{\sum_{k=1}^{m}(x_{ik}-\overline{x}_i)(x_{jk}-\overline{x}_j)}{\sqrt{\sum_{k=1}^{m}(x_{ik}-\overline{x}_i)^2 \sum_{k=1}^{m}(x_{jk}-\overline{x}_j)^2}} \quad (1)$$

The r_{ij} is the gene correlation score. For genes *i* and *j* , the expression levels in the *m-th* patient are represented as (x_{i1},x_{i2} ,... ,x_{im}) and (x_{j1},x_{j2},... ,x_{jm}) (x_{j1},x_{j2} ,... ,x_{jm}), respectively. $\overline{x}_i$ and $\overline{x}_j$ represent the average expression levels of genes *i* and *j* across all patients.

The PD-GCN at each time snapshot *p* is defined as $G_p = (V_p, E_p)$, where the vertex set V_p represents the set of genes, i.e., $V_p = g_1, g_2, \ldots, g_p$, with each gene g_i corresponding to a vertex. The edge set E_p represents the co-expression relationships between genes at time *p* , where if $r_{ij} > 1$, an edge exists between gene *i* and gene *j*.

$$E_p = \{(g_i, g_j) \mid r_{ij} > 0.1\} \tag{2}$$

3.2 Dynamic Spatial Graph Neural Network

In gene co-expression network analysis and whole blood transcriptome data processing, the interactions between genes are not static; they change with time, experimental conditions, and biological states. Traditional static graph neural networks are not capable of effectively capturing these dynamic changes, whereas dynamic graph neural networks can track changes in the graph structure and capture the dynamic characteristics of gene expression patterns over time, thereby enabling a better understanding of gene interactions under different biological conditions. Overview of dynamic graph neural networks is shown in Fig 2.

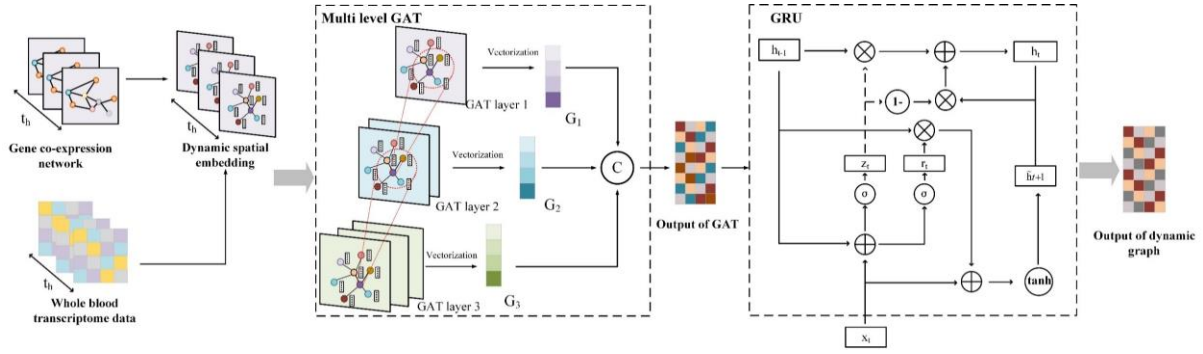

Fig 2: The architecture of Dynamic Spatial Graph Neural Network. This framework integrates multi-stage dynamic gene graphs to capture structural changes in gene networks, enabling the investigation of evolutionary mechanisms that drive disease progression.

In Fig 2, the Graph Attention Network (GAT) is used to process spatial information, while the Gated Recurrent Unit (GRU) plays a key role in dynamically updating the network parameters to capture the structural changes of the dynamic gene graph over time. Specifically, $G_t$and X_t represent the spatial and temporal information at time snapshot *t*, respectively. The gene graph *G* is then fed into the stack of GAT layers to construct multi-level graph features, thereby enhancing the dynamic spatial representation. Through this process, GAT effectively captures the complex spatiotemporal relationships between nodes in the graph over time. The attention coefficient a_{ij} is computed according to the following formula:

$$\alpha_{ij} = \frac{\exp\left(W_2\left(W_1 v_i \parallel W_1 v_j\right)\right)}{\sum_{k \in N_i} \exp\left(W_2(W_1 v_i \parallel W_1 v_k)\right)} \tag{3}$$

Where W_1 and W_2 represent the weight matrices of the fully connected layers, $\parallel$ denotes the concatenation operation, and *v* represents the nodes in the graph. $k \in N_i$ refers to the first-order neighboring nodes of node *i*. Subsequently, the attention coefficient α_{ij} is used to compute the feature output corresponding to node *i*:

$$v_i' = \sigma\left(\sum_{j \in N_i} \alpha_{ij} W_1 v_j\right) \tag{4}$$

In Eq (4), *W* represents the weight matrix, and σ denotes the non-linear activation function. This study employs a three-layer GAT (Graph Attention Network) architecture, which produces outputs G_1, G_2, and G_3, respectively. To obtain a more comprehensive spatial representation, these outputs are concatenated along the feature dimension to generate the final spatial feature X_S.

$$X_S = Concat[G_1, G_2, G_3] \tag{5}$$

To encode the dynamic gene graph and obtain the hidden states of the nodes at future time steps, the final spatial representation X_S is fed into the GRU, with its forward propagation formula defined as follows:

$$z_t = \sigma(X_S W_Z + U_Z h_{t-1}) \tag{6}$$

$$r_t = \sigma(X_S W_r + U_r h_{t-1}) \tag{7}$$

$$\widetilde{h_t} = \tanh\left(X_S W_x + U_h(r_t \cdot h_{t-1})\right) \tag{8}$$

$$h_t = (1 - z_t)h_t - 1 + z_t * \widetilde{h_t} \tag{9}$$

Where X_S represents the input vector of the *t*-th time snapshot, while W_z, W_r, W_h, U_z, U_r, and U_h are weight matrices. h_{t-1} retains the structural information of the previous time snapshot t-1, and σ denotes the non-linear activation function. X_S is linearly transformed to generate the update gate z_t and the reset gate r_t. In this process, the temporal information is preserved through the reset gate and updated as $\widetilde{h_t}$.

3.3 Dual-Channel Transformer

This section introduces a dual-channel Transformer architecture designed to establish an effective interaction mechanism between the temporal and spatial views, thereby enhancing the representation of data features.

As shown in part (B) of Fig 1, X_S represents dynamic spatial features, and X_T represents temporal features. These two features are mapped to the corresponding query (Q), key(K), and value(V) vectors through linear layers. The corresponding formulas are as follows:

$$Q = XW_q \tag{10}$$

$$K = XW_k \tag{11}$$

$$V = XW_v \tag{12}$$

$$Attention(Q_S, K_T, V_T) = softmax\left(\frac{Q_S K_T^T}{\sqrt{d_k}}\right)V_T \tag{13}$$

$$Attention(Q_T, K_S, V_S) = softmax\left(\frac{Q_T K_S^T}{\sqrt{d_k}}\right)V_S \tag{14}$$

Where W_q, W_k, and W_v are learnable parameters of different feedforward neural networks, and (Q_S, K_S, V_S) and (Q_T, K_T, V_T) are the query, key, and value corresponding to X_S and X_T, respectively. Then, the spatial and temporal features X_S and X_T generated by $\mathrm{Attention}(Q_S, K_T, V_T)$ and $\mathrm{Attention}(Q_T, K_S, V_S)$ are concatenated to obtain a consensus representation $X_{consensus}$.

$$X_{consensus} = Concat[X_S, X_T] \tag{15}$$

The fused feature $X_{consensus}$ is fed into a classifier composed of Kolmogorov-Arnold Networks (KAN) to predict the classification result.

$$\hat{y} = f_{KAN}(X_{consensus}) \tag{16}$$

Where f_{KAN} represents the KAN, and $\hat{y}$ is the predicted output. Ultimately, we compute the cross-entropy loss using $\hat{y}$ and *y* nd optimize the model using gradient descent.

$$L_{STGAT}^{(t)} = -\frac{1}{NT}\sum_{i=1}^{N}\sum_{t=1}^{T}\sum_{c=1}^{C} y_{i,t,c}\log\left(\hat{y}_{i,t,c}\right) + \lambda\sum_{j}\left\|\theta_j\right\|^2 \tag{17}$$

Where *N* epresents the number of samples, and *T* represents the number of time snapshots. $y_{i,t,c}$ denotes the true label of the *i*-th sample at time snapshot *t* belonging to class *c*, while $\hat{y}_{i,t,c}$ represents the predicted probability of the *i*-th sample at time snapshot *t*. A regularization term, $\lambda\sum_j|\theta_j|^2$, is introduced into the original loss function to maintain the balance between the two penalty terms.

4. EXPERIMENTAL OUTCOMES AND ANALYSIS

4.1 Datasets

Experiments were conducted on two real datasets, PPMI and PDBP. The data is represented as two-dimensional matrices, where the rows correspond to patient IDs and the columns correspond to gene IDs. The labels are derived from the Hoehn & Yahr (H&Y) [29] staging included in the Unified Parkinson's Disease Rating Scale (UPDRS) [30]. H&Y staging is a clinical tool for assessing motor function in Parkinson's disease, consisting of five stages that describe disease progression from mild unilateral symptoms to severe bedbound dependency: Stage 1 represents mild unilateral symptoms without affecting daily activities; Stage 2 involves bilateral symptoms without postural instability; Stage 3 is characterized by postural instability while retaining independent living; Stage 4 indicates severe functional disability requiring assistance; and Stage 5 corresponds to bedridden or wheelchair dependency with loss of independent living.

In the PDBP dataset, 385 patients were included, and data collected at 6 months (M6), 12 months (M12), and 18 months (M18) post-baseline was used to predict the H & Y staging at 24 months (M24). In the PPMI dataset, 203 patients were included, and data collected at 6 months (M6), 12 months (M12), and 24 months (M24) post-baseline was used to predict the H&Y staging at 36 months (M36). For both datasets, the top 500 most variable genes were selected to construct dynamic gene graphs. The detailed information is shown in Table I.

TABLE I: Dataset description

Dataset	Source	Samples	Features	Nodes	Visits	Edges
PPMI	Whole blood data	278	58780	500	M6	1470
					M12	1447
					M24	1469
					M36	1467
PDBP	Whole blood data	278	58780	500	M6	1459
					M12	1440
					M18	1447
					M24	1450

4.2 Implementation Details

All experiments were implemented and evaluated on an NVIDIA GeForce RTX 4090 GPU. For model training, we utilized the AdamW [31] optimizer, with learning rates tuned to 0.000001, 0.00001, and 0.0001. The cross-entropy loss function was employed for loss computation. In our experiments, the graph neural network adopted a three-layer GAT model with attention heads set to 4, 3, and 4, respectively. Additionally, the dual-channel Transformer model used 8 attention heads.

In this study, four effectiveness metrics were employed to evaluate the performance of the prediction model: Accuracy (Acc), F1-score(F1), Recall(Rec), and Precision(Pre). Additionally, to mitigate the impact of random initialization, five-fold cross-validation is conducted for all experiments, and the average results are utilized for comparison.

$$Acc = \frac{TP + TN}{TP + TN + FP + FN} \tag{18}$$

$$Rec = \frac{TP}{TP + FN} \tag{19}$$

$$Pre = \frac{TP}{TP + FP} \tag{20}$$

$$F1 = \frac{2 \times Pre \times Rec}{Pre + Rec} \tag{21}$$

Where TP, TN, FP, and FN represent the number of true positive cases, true negative cases, false positive cases, and false negative cases, respectively.

4.3 Inference of dynamic gene graph

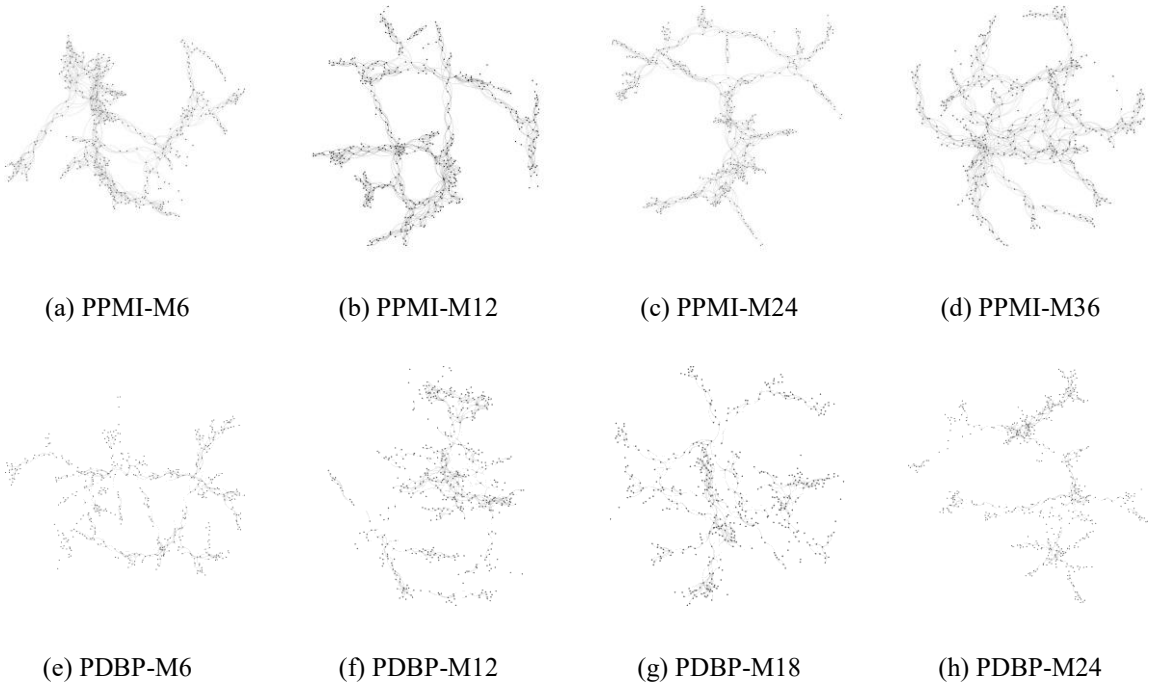

(a) PPMI-M6 (b) PPMI-M12 (c) PPMI-M24 (d) PPMI-M36

(e) PDBP-M6 (f) PDBP-M12 (g) PDBP-M18 (h) PDBP-M24

Fig 3: The topological structures of PD-GCN at different disease stages were visualized. For the PPMI cases, these stages include follow-ups at 6 months (M6), 12 months (M12), 24 months (M24), and 36 months (M36) after the onset of Parkinson's disease. Using a Parkinson's disease progression prediction model, the study investigates the relationship between changes in gene network topologies and the H&Y staging scale.

In Fig 3, it can be observed that over time, the gene co-expression network for Parkinson's disease (PD-GCN) gradually becomes more complex and chaotic, with increasingly intricate relationships between genes. For example, in the case of PDBP, in the early stages (M6), the network structure remains relatively stable, and the interactions between genes are balanced. This stage represents the onset of the disease, where, despite the beginning of neurodegenerative damage, the overall gene regulatory network has not yet experienced significant disruption, and the gene co-expression relationships remain stable. However, over time, particularly in the middle stages (M12, M24) and the later stage (M36), the gene co-expression network becomes more complex and disordered. This change reflects the degenerative alterations in neural cells and the gradual loss of synaptic function, leading to more complex regulatory relationships between genes. As the disease advances, neurons in the nervous system progressively lose function, and the connectivity between neurons, as well as gene expression, changes, which in turn leads to instability and disorder in the network structure. During this process, the interactions between genes become imbalanced, with some genes being excessively activated or suppressed, thereby exacerbating neurodegenerative changes. This transformation not only reflects the molecular progression of the disease but also highlights the trend of increasing severity of neurodegenerative diseases with age.

4.4 Performance comparison

This study presents a network architecture called Dynamic Spatiotemporal Graph Learning (DST-GNN), aimed at investigating subtle variations in blood expression data and topological distortions in gene graphs for predicting short-term disease progression. To validate the effectiveness of the proposed method, comparative experiments were conducted on multiple public datasets, and its performance was compared with state-of-the-art baseline methods. These methods briefly presented as below:

- FC-LSTM [32]: FC-LSTM introduces fully connected layers on top of the LSTM, enabling the model to effectively integrate information at each time step and capture both short-term and long-term dependencies in the time series.
- Transformer [33]: Transformer effectively captures complex nonlinear relationships and long-term dependencies in the sequence through its self-attention mechanism.
- MLA-GNN [34]: The Multi-level Attention Graph Neural Network is a graph neural network that uses gene co-expression networks as input.
- STGAT [35]: Spatial-Temporal Graph Attention Networks use the graph attention mechanism to capture spatial dependencies in the graph, while incorporating an LSTM network to extract temporal features.
- STS-DGNN [36]: The Dynamic Graph Neural Network with Spatial-Temporal Synchronization fully considers the dynamics of graph sequences.

TABLE II: Comparison of evaluation metrics obtained by DST-GNN and candidate PD progression prediction methods.

Datasets	Method	Acc	F1	Rec	Pre
PPMI	FC-LSTM [32]	0.672 ± 0.009	0.546 ± 0.005	0.669 ± 0.009	0.463 ± 0.001
	Transformer [33]	0.663 ± 0.013	0.541 ± 0.012	0.659 ± 0.014	0.457 ± 0.006
	MLA-GNN [34]	0.673 ± 0.011	0.572 ± 0.028	0.672 ± 0.011	0.647 ± 0.040
	STGAT [35]	0.675 ± 0.019	0.595 ± 0.039	0.678 ± 0.019	0.707 ± 0.014
	STS-DGNN [36]	0.679 ± 0.024	0.617 ± 0.041	0.684 ± 0.023	0.697 ± 0.036
	DST-GNN(Ours)	**0.749 ± 0.013**	**0.718 ± 0.009**	**0.748 ± 0.017**	**0.784 ± 0.025**
PDBP	FC-LSTM	0.650 ± 0.009	0.518 ± 0.006	0.649 ± 0.007	0.432 ± 0.013
	Transformer	0.633 ± 0.008	0.504 ± 0.001	0.615 ± 0.044	0.438 ± 0.026
	MLA-GNN	0.685 ± 0.006	0.595 ± 0.017	0.687 ± 0.006	0.721 ± 0.008
	STGAT	0.683 ± 0.005	0.590 ± 0.021	0.684 ± 0.006	0.725 ± 0.007
	STS-DGNN	0.691 ± 0.008	0.611 ± 0.023	0.691 ± 0.005	0.730 ± 0.005
	DST-GNN(Ours)	**0.744 ± 0.009**	**0.710 ± 0.012**	**0.744 ± 0.008**	**0.770 ± 0.011**

Table II presents a detailed comparison of DST-GNN with other candidate prediction methods across various evaluation metrics. Meanwhile, Fig 4 illustrates the ROC curve comparison of the respective candidate methods. We can categorize the models into two types. The first type consists of single-view models, such as FC-LSTM, Transformer, and MLA-GNN. Among them, FC-LSTM and Transformer utilize only blood transcriptomics data, while MLA-GNN is based solely on gene co-expression network graphs. The second type includes dual-view spatiotemporal collaborative models, such as STGAT and STS-DGNN, which simultaneously leverage blood transcriptomics data and gene graphs. Research indicates that models trained on gene graphs outperform those trained solely on blood transcriptomics data, demonstrating the critical value of gene graphs as spatial features in disease evolution modeling. Furthermore, dual-view spatiotemporal collaborative models, which integrate the spatial distribution and temporal dynamics of the data, significantly outperform models that rely solely on temporal or spatial information. Our model, by fusing the dynamic changes in gene expression patterns with the topological features of the co-expression network, provides a more precise representation of gene regulatory mechanisms and identifies key regulatory factors. Compared to all baseline methods, our model achieves superior performance across all evaluation metrics.

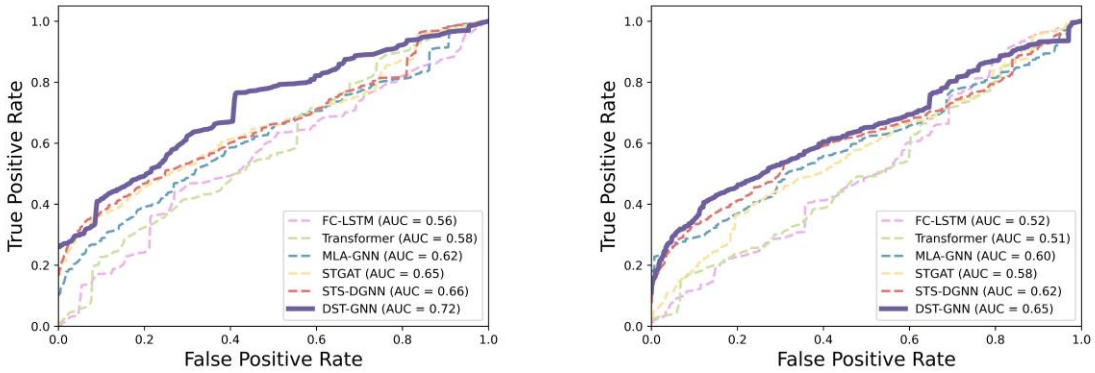

(a) PPMI (b) PDBP

Fig 4: Performance comparison of DST-GNN with other baseline methods

4.5 Ablation study

As shown in Table III, ablation experiments were designed to assess the impact of each component on model performance. The experiments include three different configurations: (i) DST-GNN without dynamic spatial GNN, (ii) DST-GNN without the dual-channel Transformer, using concatenation for spatiotemporal feature fusion, and (iii) DST-GNN without KNN, using a standard fully connected layer as the classifier.

TABLE III: Ablation analysis for DST-GNN

Dynamic Spatial GNN	Dual-Channel Transformer	KAN	PPMI				PDBP			
			Acc	F1	Rec	Pre	Acc	F1	Rec	Pre
	√	√	0.743	0.719	0.717	0.730	0.690	0.614	0.691	0.734
√	√		0.748	0.721	0.744	0.792	0.741	0.692	0.743	0.771
√		√	0.758	0.728	0.759	0.809	0.760	0.720	0.755	0.775
√	√	√	**0.761**	**0.733**	**0.762**	**0.820**	**0.763**	**0.726**	**0.765**	**0.785**

From Table III, it can be observed that the dynamic spatial GNN component has the most significant impact on the performance of the DST-GNN model compared to the other two components, with an average increase of 9.5% in accuracy (ACC) across both datasets. This component is capable of dynamically updating the nodes and edges in the gene co-expression network, allowing it to capture subtle changes in real time. Furthermore, the dual-channel Transformer architecture and the KAN structure also significantly improve the accuracy of PD progression prediction. While traditional spatio-temporal collaborative models consider the dynamics of the graph, they overlook changes in gene expression levels. In contrast, DST-GNN, through the dual-channel Transformer, effectively captures the relationships and interactions between gene expression and graph dynamics. Moreover, the KAN structure, compared to fully connected layers, better captures the complex dependencies in the temporal sequence, thereby enhancing the model's ability to predict disease progression and gene dynamic changes.

5. CONCLUSION

Based on whole-blood RNA-seq data, the proposed DST-GNN method is effective to conduct progression prediction for Parkinson's disease(PD). Under the framework of spatiotemporal learning, blood expression levels and dynamic gene graphs have been integrated to boost model performance in investigating motor dysfunction process of PD. As a kind of spatial feature, gene graphs are proven to valuable in disease modeling. The DST-GNN has achieved superior performance than conventional ST-GNN and dynamic GNN, validating the effectiveness and advantage of dynamic gene graphs. It is noted that dynamic gene graphs are more informative than static graphs, by capturing evolving patterns of molecular networks.

REFRENCES

[1] Mostafavi S, Gaiteri C, Sullivan S E, et al. A molecular network of the aging human brain provides insights into the pathology and cognitive decline of Alzheimer's disease[J]. Nature neuroscience, 2018, 21(6): 811-819.

[2] Johnson E C B, Carter E K, Dammer E B, et al. Large-scale deep multi-layer analysis of Alzheimer's disease brain reveals strong proteomic disease-related changes not observed at the RNA level[J]. Nature neuroscience, 2022, 25(2): 213-225.

[3] Tekin A, Nebli A, Rekik I. Recurrent brain graph mapper for predicting time-dependent brain graph evaluation trajectory[C]//MICCAI Workshop on Domain Adaptation and Representation Transfer. Cham: Springer International Publishing, 2021: 180-190.

[4] Exley T, Moudy S, Patterson R M, et al. Predicting UPDRS motor symptoms in individuals with Parkinson's disease from force plates using machine learning[J]. IEEE Journal of Biomedical and Health Informatics, 2022, 26(7): 3486-3494.

[5] Harvey J, Reijnders R A, Cavill R, et al. Machine learning-based prediction of cognitive outcomes in de novo Parkinson's disease[J]. npj Parkinson's Disease, 2022, 8(1): 150.

[6] Johansson M E, van Lier N M, Kessels R P C, et al. Two-year clinical progression in focal and diffuse subtypes of Parkinson's disease[J]. npj Parkinson's Disease, 2023, 9(1): 29.

[7] Craig D W, Hutchins E, Violich I, et al. RNA sequencing of whole blood reveals early alterations in immune cells and gene expression in Parkinson's disease[J]. Nature Aging, 2021, 1(8): 734-747.

[8] Irmady K, Hale C R, Qadri R, et al. Blood transcriptomic signatures associated with molecular changes in the brain and clinical outcomes in Parkinson's disease[J]. Nature Communications, 2023, 14(1): 3956.

[9] Phongpreecha T, Cholerton B, Mata I F, et al. Multivariate prediction of dementia in Parkinson's disease[J]. npj Parkinson's Disease, 2020, 6(1): 20.

[10] Kline A, Wang H, Li Y, et al. Multimodal machine learning in precision health: A sco** review[J]. npj Digital Medicine, 2022, 5(1): 171.

[11] Langfelder P, Horvath S. WGCNA: an R package for weighted correlation network analysis[J]. BMC bioinformatics, 2008, 9: 1-13.

[12] Song W M, Zhang B. Multiscale embedded gene co-expression network analysis[J]. PLoS computational biology, 2015, 11(11): e1004574.

[13] Li H, Sun Y, Hong H, et al. Inferring transcription factor regulatory networks from single-cell ATAC-seq data based on graph neural networks[J]. Nature Machine Intelligence, 2022, 4(4): 389-400.

[14] Van de Sande B, Flerin C, Davie K, et al. A scalable SCENIC workflow for single-cell gene regulatory network analysis[J]. Nature protocols, 2020, 15(7): 2247-2276.

[15] Zhang M, Wu S, Yu X, et al. Dynamic graph neural networks for sequential recommendation[J]. IEEE Transactions on Knowledge and Data Engineering, 2022, 35(5): 4741-4753.

[16] Tang X, Wang J, Liu B, et al. A comparison of the functional modules identified from time course and static PPI network data[J]. BMC bioinformatics, 2011, 12: 1-15.

[17] Liu J, Xu C, Yin C, et al. K-core based temporal graph convolutional network for dynamic graphs[J]. IEEE Transactions on Knowledge and Data Engineering, 2020, 34(8): 3841-3853.

[18] Guo S, Lin Y, Feng N, et al. Attention based spatial-temporal graph convolutional networks for traffic flow forecasting[C]//Proceedings of the AAAI conference on artificial intelligence. 2019, 33(01): 922-929.

[19] Diao Z, Wang X, Zhang D, et al. Dynamic spatial-temporal graph convolutional neural networks for traffic forecasting[C]//Proceedings of the AAAI conference on artificial intelligence. 2019, 33(01): 890-897.

[20] Wang J, Gao Y, Wang F, et al. Accurate estimation of biological age and its application in disease prediction using a multimodal image Transformer system[J]. Proceedings of the National Academy of Sciences, 2024, 121(3): e2308812120.

[21] Xu J, Huang D S, Zhang X. scmFormer integrates large-scale single-cell proteomics and transcriptomics data by multi-task transformer[J]. Advanced Science, 2024, 11(19): 2307835.

[22] Zhou H Y, Yu Y, Wang C, et al. A transformer-based representation-learning model with unified processing of multimodal input for clinical diagnostics[J]. Nature Biomedical Engineering, 2023, 7(6): 743-755.

[23] **e Y, Zhang Y, Gong M, et al. Mgat: Multi-view graph attention networks[J]. Neural Networks, 2020, 132: 180-189.

[24] Jiang W B, Liu X H, Zheng W L, et al. Multimodal adaptive emotion transformer with flexible modality inputs on a novel dataset with continuous labels[C]//proceedings of the 31st ACM international conference on multimedia. 2023: 5975-5984.
[25] Huang H, Song Y, Wu Y, et al. Multitask representation learning with multiview graph convolutional networks[J]. IEEE Transactions on Neural Networks and Learning Systems, 2020, 33(3): 983-995.
[26] Wang Q, Zhang Y, Wang M, et al. The landscape of multiscale transcriptomic networks and key regulators in Parkinson's disease[J]. Nature communications, 2019, 10(1): 5234.
[27] Yang D, ** Y, He X, et al. Inferring multilayer interactome networks sha** phenotypic plasticity and evolution[J]. Nature Communications, 2021, 12(1): 5304.
[28] Barrio-Hernandez I, Schwartzentruber J, Shrivastava A, et al. Network expansion of genetic associations defines a pleiotropy map of human cell biology[J]. Nature genetics, 2023, 55(3): 389-398.
[29] Bhidayasiri R, Tarsy D, Bhidayasiri R, et al. Parkinson's disease: Hoehn and Yahr scale[J]. Movement disorders: a video atlas: a video atlas, 2012: 4-5.
[30] Goetz C G, Tilley B C, Shaftman S R, et al. Movement Disorder Society-sponsored revision of the Unified Parkinson's Disease Rating Scale (MDS-UPDRS): scale presentation and clinimetric testing results[J]. Movement disorders: official journal of the Movement Disorder Society, 2008, 23(15): 2129-2170.
[31] Loshchilov I, Hutter F. Fixing weight decay regularization in adam[J]. arxiv preprint arxiv:1711.05101, 2017, 5: 5.
[32] Yu Y, Si X, Hu C, et al. A review of recurrent neural networks: LSTM cells and network architectures[J]. Neural computation, 2019, 31(7): 1235-1270.
[33] Wu N, Green B, Ben X, et al. Deep transformer models for time series forecasting: The influenza prevalence case[J]. arxiv preprint arxiv:2001.08317, 2020.
[34] **ng X, Yang F, Li H, et al. Multi-level attention graph neural network based on co-expression gene modules for disease diagnosis and prognosis[J]. Bioinformatics, 2022, 38(8): 2178-2186.
[35] Zhang C, James J Q, Liu Y. Spatial-temporal graph attention networks: A deep learning approach for traffic forecasting[J]. Ieee Access, 2019, 7: 166246-166256.
[36] Li F J, Zhang C Y, Chen C L P. STS-DGNN: Vehicle trajectory prediction via dynamic graph neural network with spatial–temporal synchronization[J]. IEEE Transactions on Instrumentation and Measurement, 2023, 72: 1-13.